Direct detection of WIMPs
December 2018

- **Program:**
  - Principles of direct detection
    - Characteristics and signatures of dark matter
    - Cross sections for scattering on nucleons and form factors
    - Generic result of a dark matter experiment
  - Background sources, statistics and calibration of dark matter detectors
    - Sources of background: external and internal
    - Detector signals and background reduction
    - Statistical treatment of data
    - Detector calibration: energy scale and signal/background regions
  - Technologies and results of direct dark-matter searches
    - Room temperature detectors: scintillator crystals and germanium detectors
    - Cryogenic bolometers
    - Liquid noble-gas detectors
    - Superheated fluids
    - Directional searches

- **Literature:**
  - T. Marrodán Undagoitia and L. Rauch, *Dark matter direct-detection experiments*, J. Phys. G: 43 (2016) 1, arXiv:1509.08767
  - M. W. Goodman and E. Witten, *Detectability of certain dark-matter candidates*, Phys. Rev. D 31 (1985) 12
  - J. D. Lewin and P. F. Smith, *Review of mathematics, numerical factors, and corrections for dark matter experiments based on elastic nuclear recoil*, Astrop. Phys. 6 (1996) 87
  - A.K. Drukier, K. Freese and D. N. Spergel, *Detecting cold dark-matter candidates*, Phys. Rev. D 33 (1986) 12
  - D. N. Spergel, *The Motion of the Earth and the Detection of Wimps*, Phys. Rev. D37 (1988) 1353
  - K. Freese *et al*, *Colloquium: Annual modulation of dark matter*, Rev. Mod. Phys. 85 (2013) 1561, arXiv:1209.3339
  - G. Heusser, *Low-radioactivity background techniques*, Annu. Rev. Nucl. Part. Sci. **45** (1995) 543
  - L. E. Strigari, *Neutrino Coherent Scattering Rates at Direct Dark Matter Detectors*, New J. Phys. **11** (2009) 105011, arXiv:0903.3630.
  - G. J. Feldman and R. D. Cousins, *A Unified Approach to the Classical Statistical Analysis of Small Signals*, Phys. Rev. **D57** (1998) 3873 , arXiv:physics/9711021

- W. R. Leo, *Techniques for Nuclear and Particle Physics Experiments*, Springer-Verlag, 1987
- R. Bernabei et al., *First model independent results from DAMA/LIBRA-phase2*, arXiv:1805.10486
- N. Booth et al., *Low-temperature particle detectors*, A. Rev. Nucl. Part. Sci. 46 (1996) 471
- R. Agnese et al. (SuperCDMS Collaboration), *Search for Low-Mass Weakly Interacting Massive Particles with SuperCDMS*, Phys. Rev. Lett. 112 (2014) 241302
- G. Angloher et al., (CRESST Collaboration), *Results on light dark matter particles with a low-threshold CRESST-II detector*, Eur. Phys. J. C76 (2016) 25, arXiv:1509.01515
- E. Aprile and T. Doke, *Liquid xenon detectors for particle physics and astrophysics*, Rev. Mod. Phys.82 (2010) 2053, arXiv: 0910.4956
- D.S. Akerib et al. (LUX Collaboration), *Results from a search for dark matter in the complete LUX exposure*, Phys. Rev. Lett. 118 (2017) 021303, arXiv:1608.07648
- E. Aprile et al. (XENON1T Collaboration), *Dark Matter Search Results from a One Ton-Year Exposure of XENON1T*, Phys. Rev. Lett. 121 (2018) no.11, 111302 , arXiv:1805.12562
- C. Amole et al. (PICO Collaboration), *Dark Matter Search Results from the PICO-60 C_3F_8 Bubble Chamber*, Phys. Rev. Lett. 118 (2017) 251301, arXiv:1702.07666
- J. Billard *et al.*, *Directional detection as a strategy to discover Galactic dark matter*, Phys. Lett. B 691 (2010) 156

- **Material for the lecture:**

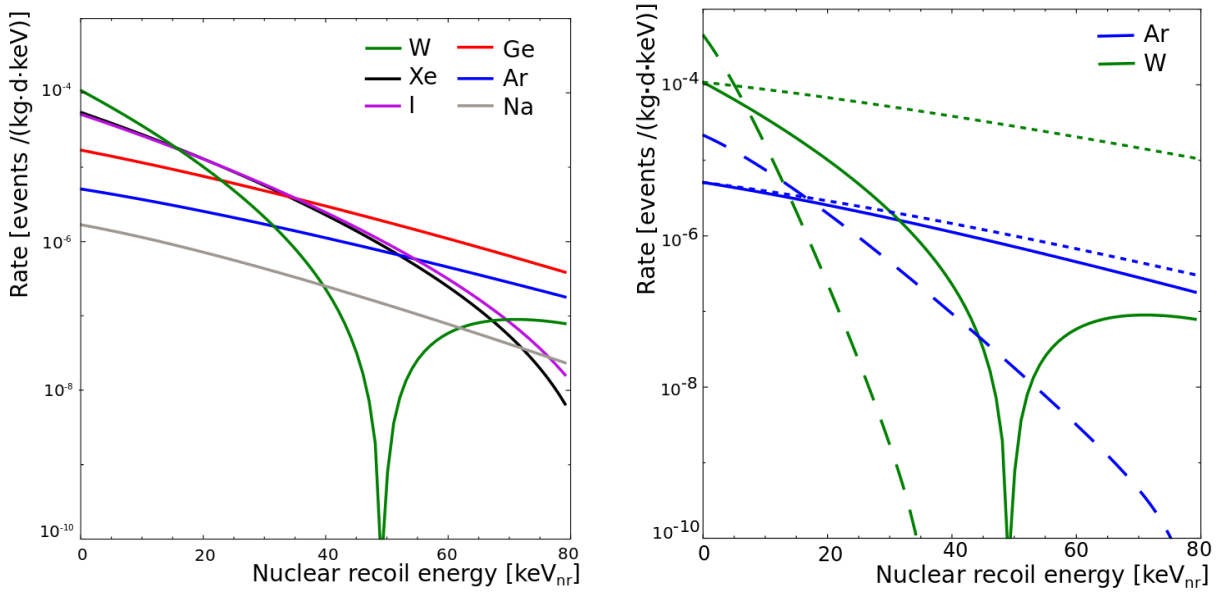

Figure 1: (Left) Event rates as function of nuclear recoil energy for different target materials assuming a 100 GeV/c^2 WIMP mass and an interaction cross section of 10^{-45} cm^2 (solid lines). (Right) Event rates for argon and tungsten. Dotted line: no form factor correction. Dashed line: for a 25 GeV/c^2 WIMP mass. Figures from arXiv:1509.08767.

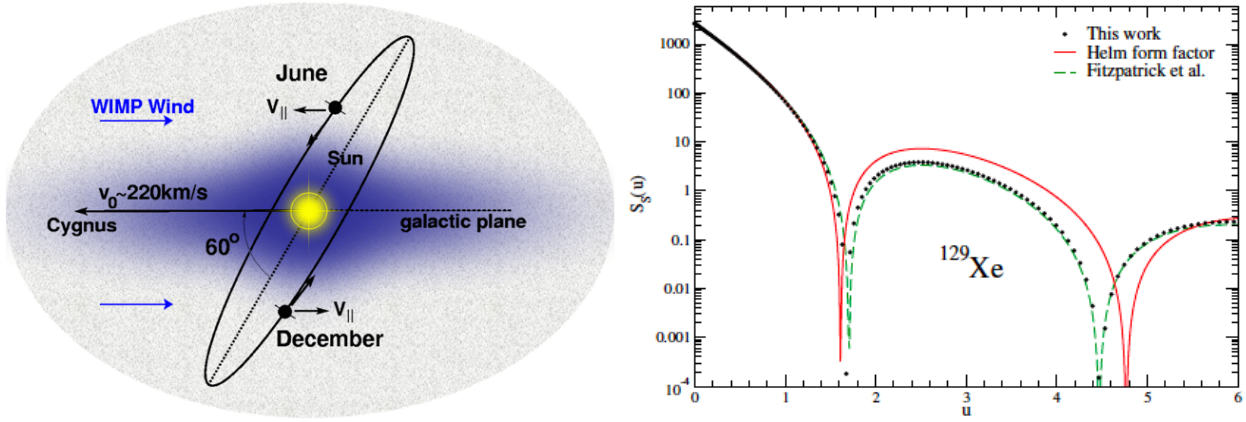

Figure 2: Left: Scheme of the kinematic that give an annual modulation of the dark matter rate. Right: Structure factor $S_S(u)$ for ^{129}Xe (black dots) in comparison with the Helm form factor (red) and the Fitzpatrick structure factor. Figure from L. Vietze et al. PRD 91 (2015) 043520 and arXiv:1412.609.

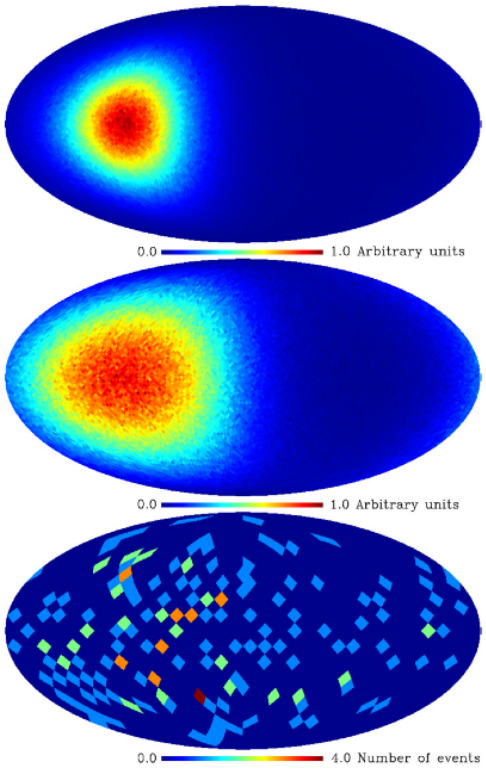

Figure 3: Directionality signature: (top) WIMP flux in the case of an isothermal spherical halo, (middle) WIMP-induced recoil distribution and (bottom) a typical simulated measurement: 100 WIMP recoils and 100 background events (low angular resolution). Figure from J. Billard et al. 2010.

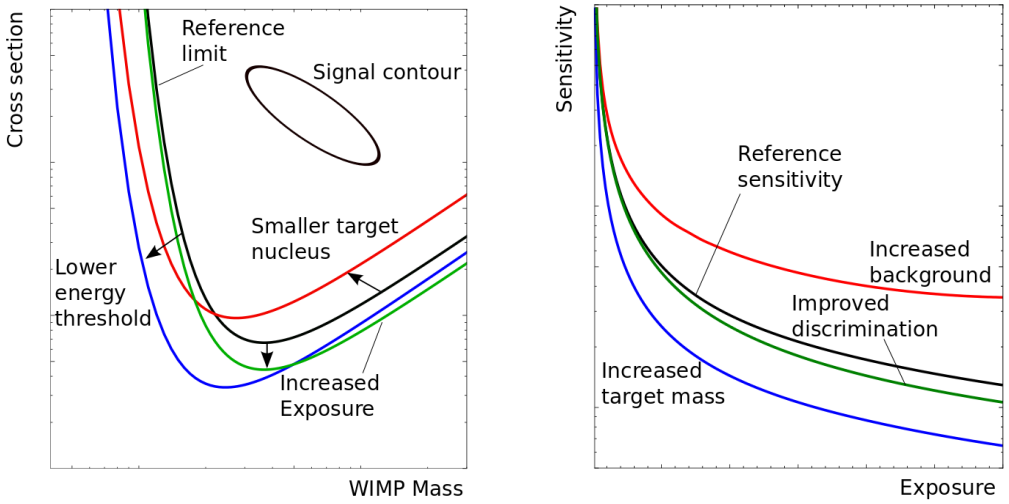

Figure 4: Sensitivity of direct detection experiments for different parameters. From arXiv:1509.08767.

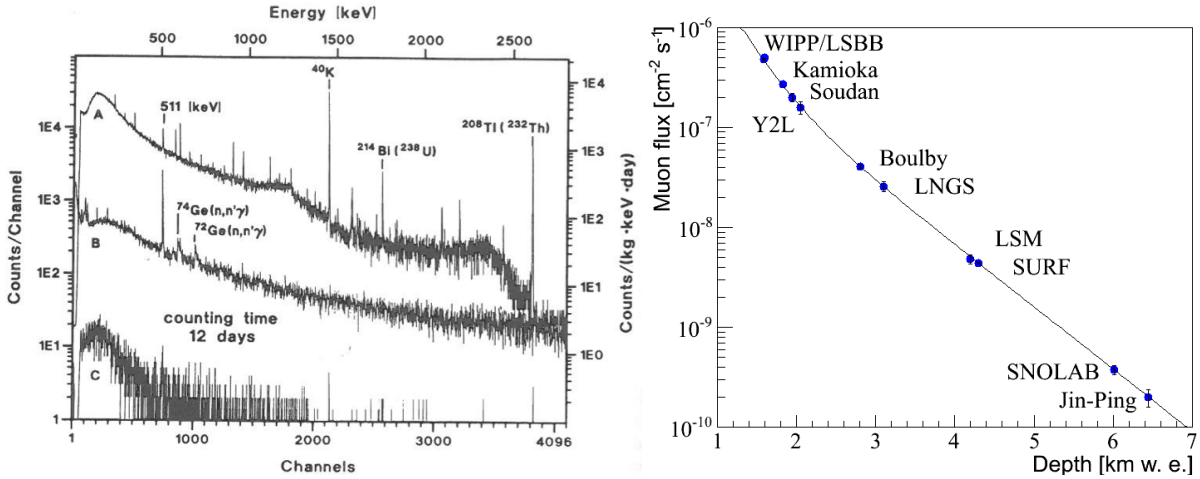

Figure 5: Left: Background spectra of a Ge detector without shield (top), with 15 cm lead shield (middle), and with shield and at 500 m.w.e. (bottom). Right: Muon flux measured for the various underground sites as function of the equivalent vertical depth. Figure from arXiv:1509.0876.

Figure 6: Examples of detector shielding, DAMA detector (left) and XENON100 detector (right).

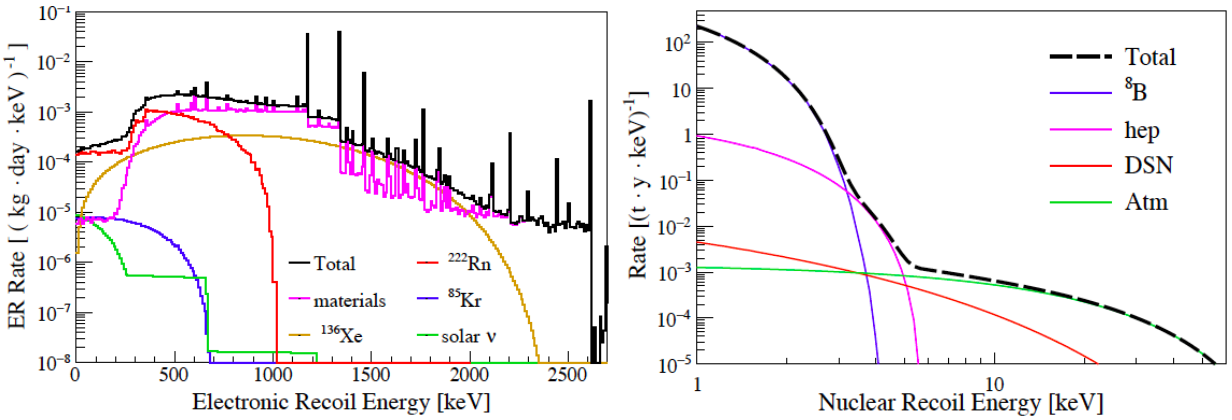

Figure 7: (Left) Contributions of different background sources to the ER region for XENON1T. (Right) Spectral shape of coherent neutrino scattering in xenon. Figures from XENON Coll., arXiv:1512.07501.

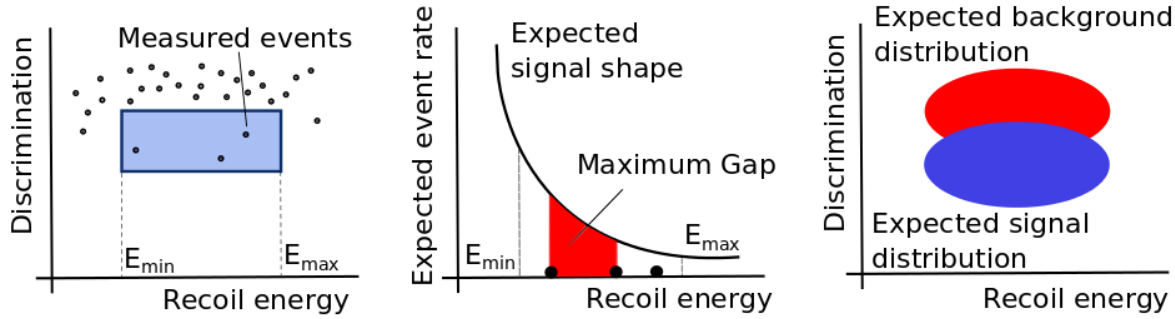

Figure 8: Illustration of different statistical methods used to derive results from direct detection experiments. Figure from arXiv:1509.08767.

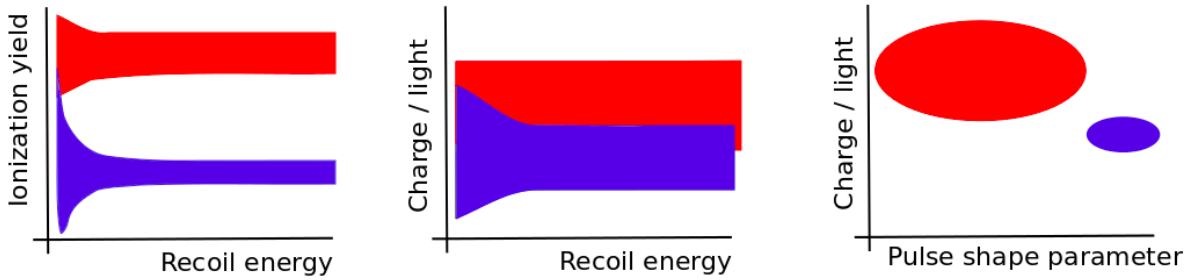

Figure 9: Schematic representation for the calibration of signal and background regions for different types of detectors: germanium (left), LXe (middle) and LAr (right). Figures from arXiv:1509.08767.

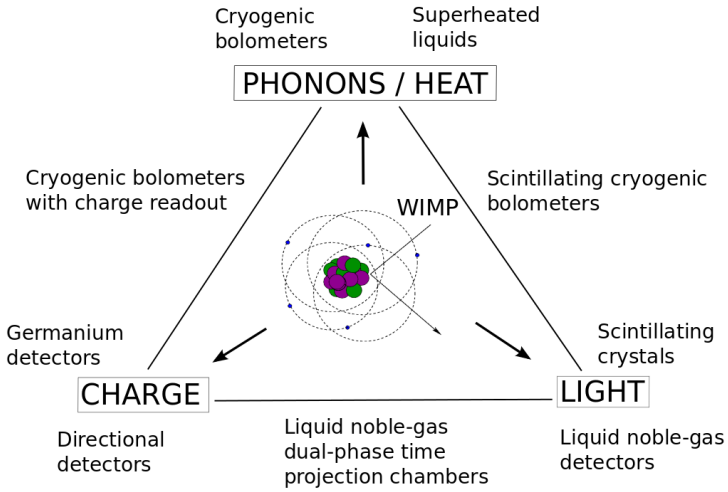

Figure 10: Schematic of signals in different detection technologies. From arXiv:1509.08767.

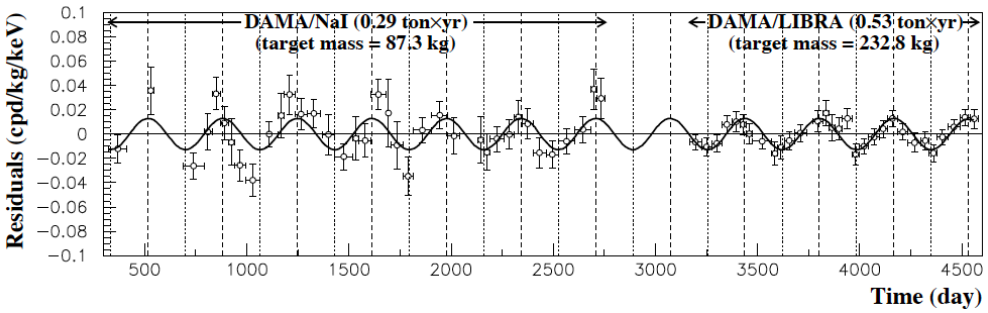

Figure 11: Residual rate of single-hit scintillation events by the DAMA/LIBRA experiment in the $(2-6)$ keV energy region as a function of time. Figure from DAMA Coll., EPJC56 (2008) 333.

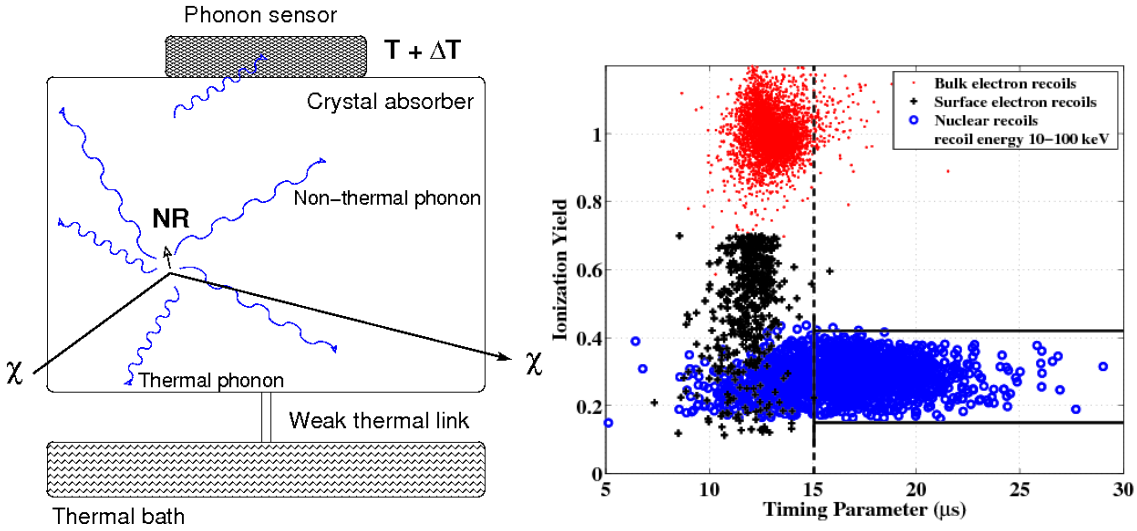

Figure 12: Left: Schematic representation of a cryogenic bolometer. Right: Ionisation yield and timing parameter for electronic recoils, nuclear recoils and surface events. Figure from CDMS Coll., Phys. Rev. Lett. 102 (2009) 011301.

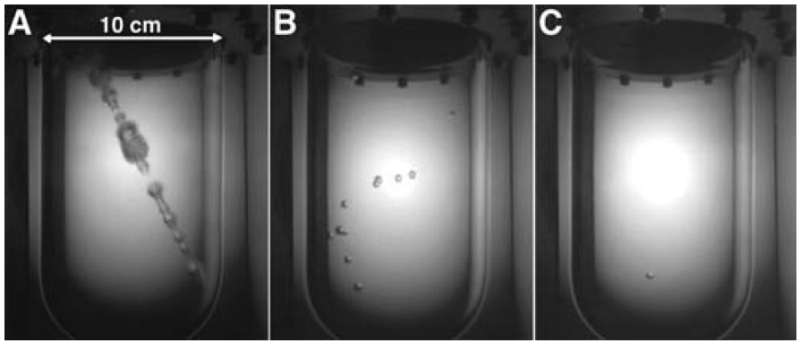

Figure 13: Events in a superheated-liquid bubble chamber (1.5 kg of CF_3I). A: muon track, B: nuclear recoils from neutrons, C: expected signature of a WIMP interaction, a single nuclear recoil bubble. Figure from E. Behnke et al., Science 319 (2008) 933.

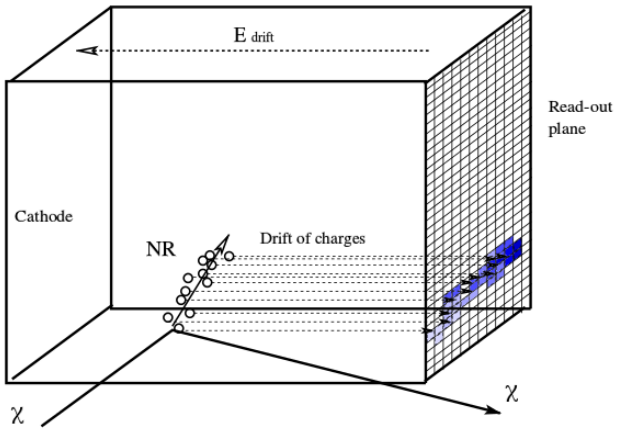

Figure 14: Schematic representation of the detection principle for cryogenic bolometers (left) and for directional detectors (right). Figure from arXiv:1509.08767.

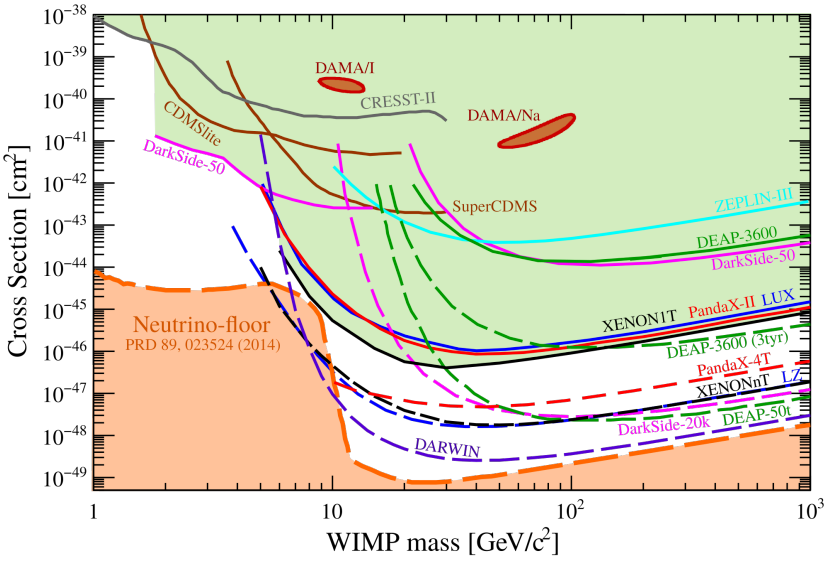

Figure 15: Spin-independent direct detection results: solid curves represent published results while dashed lines are projections for the future. Neutrino floor represented in orange.